Visualization of biochemical networks in living cells

Ingrid Remy and Stephen W. Michnick*

Département de Biochimie, Université de Montréal, C.P. 6128, Succursale centre-ville, Montréal, QC, Canada H3C 3J7

Functional annotation of novel genes can be achieved by detection of interactions of their encoded proteins with known proteins followed by assays to validate that the gene participates in a specific cellular function. We report an experimental strategy that allows for detection of protein interactions and functional assays with a single reporter system. Interactions among biochemical network component proteins are detected and probed with stimulators and inhibitors of the network. In addition, the cellular location of the interacting proteins is determined. We used this strategy to map a signal transduction network that controls initiation of translation in eukaryotes. We analyzed 35 different pairs of full-length proteins and identified 14 interactions, of which five have not been observed previously, suggesting that the organization of the pathway is more ramified and integrated than previously shown. Our results demonstrate the feasibility of using this strategy in efforts of genomewide functional annotation.

Rapid progress in genome projects is leading to the identification or prediction of a huge number of genes, but only a fraction of gene functions can be inferred from primary gene sequences. A first step in defining the function of a gene is to determine its interactions with other gene products. This is the basis of the highly successful yeast two-hybrid system (1, 2). The second step is to perform functional assays in model cells or whole organisms from which the genes in question were derived. It would be advantageous if one could combine screening of protein–protein interactions with tests for biological relevance by using a single assay system, thus validating the screening results and eliminating spurious interactions immediately. Therefore, we developed an experimental approach for detecting protein–protein interactions in intact living cells on the basis of protein interaction-induced folding and reconstitution of the activity of the enzyme murine dihydrofolate reductase (DHFR) from two rationally dissected fragments of the enzyme (3–6). In general, we call this, and other assays we have developed based on the same principle, protein fragment complementation assays (PCA) (6). We have demonstrated that the DHFR PCA can be used as a sensitive survival-selection assay and also as a fluorescence assay that allows for quantitative detection of induced protein–protein interactions (4, 5). In this report, we describe a strategy and a proof of principle for the use of the DHFR PCA in functional validation of protein interactions and mapping of biochemical pathways.

In defining our strategy we needed to answer the following question. If we observe an interaction between two proteins in a simple screen (survival-selection assay), what additional information must we generate, for example, using the fluorescence assay, to show that the interaction is biologically relevant? Fig. 1*A* provides a scheme for understanding the organization of proteins within signal transduction pathways.

Signal transduction pathways have proven useful models for examining the organization of biochemical pathways and networks for the following reasons. First, signal transduction pathways have defined initiation events, such as hormone activation of a membrane receptor, and thus in principle it is straightforward to define the quiescent and stimulated states of the pathway. Second, the position of a specific interaction within a series of events in a signaling cascade can be determined by examining the effects of agents that inhibit known steps in the pathway. The agents could include specific small molecule inhibitors, dominant-negative mutants, or antisense RNA for individual components of the pathway. Observing induction and inhibition of individual protein–protein interactions in a signaling cascade would provide functional validation in the following ways: (*i*) Perturbation of protein–protein interactions in predicted ways by hormones and inhibitors would provide convincing evidence that the proteins participate in the pathway. (*ii*) The way in which the stimulators and inhibitors affect an interaction (the "pharmacological profile") would provide evidence for the position of the particular interaction within the pathway. (*iii*) Signal transduction pathways are hierarchically organized in space, with early events occurring at the inner membrane surface, whereas later events may occur in the cytosol, nucleus, or other subcellular compartments. A biologically relevant protein–protein interaction must occur at a surface or within a cellular compartment that is consistent with its position within the signaling cascade.

In this report, we demonstrate that screening, pharmacological profiling, and the cellular location of protein–protein interactions can be achieved by using the survival-selection and fluorescence DHFR PCA. As a proof of principle, we studied a signal transduction pathway involved in insulin and growth factor receptor tyrosine kinase (RTK)-mediated control of initiation of translation in eukaryotes (Fig. 1*B*). We also studied a parallel pathway that both cross-talks with the RTK pathway and affects the proteins involved with initiation of translation that converge with the RTK pathway. This pathway is controlled by the serine/threonine kinase FK506-binding protein (FKBP)-rapamycin-associating protein (FRAP) (7, 8).
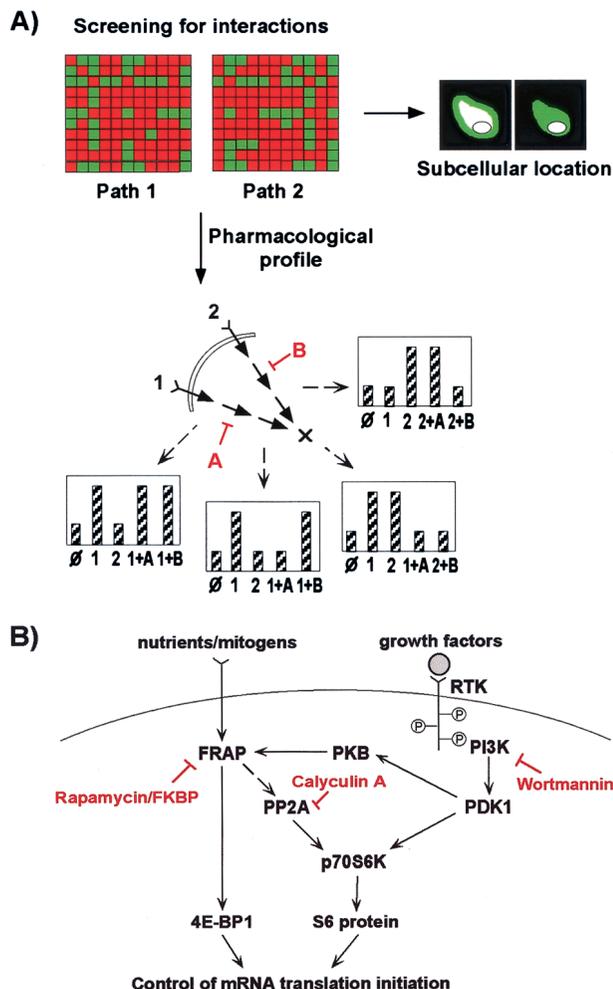
Materials and Methods

DNA Constructs. The full-length cDNAs encoding protein kinase B (PKB) and PKB(K→A), 3-phosphoinositide-dependent protein kinase 1 (PDK1), S6 ribosomal protein kinase (p70S6K) and p70S6K(K→A), S6 ribosomal protein, FRAP and FRAP(D→A), eIF-4E-binding protein (4EBP1), FKBP, the α catalytic subunit of protein phosphatase 2A (PP2A), and the GTPases Cdc42hs and Rac1 were amplified by PCR and subcloned into the eukaryotic expression vector pMT3 (9), in 5′ or 3′ of the F[1,2:F31S], which we call F[1, 2], and the F[3] fragment of DHFR (4). F (1, 2) corresponds to amino acids 1 to 105 and F[3] to amino acids 106 to 186 of murine DHFR. In all cases, a 10-aa flexible linker consisting of (Gly.Gly.Gly.Gly.Ser)$_2$ was inserted between the cDNA and the DHFR fragments. The ZIP-F[1, 2] and ZIP-F[3] constructs (described in ref. 4) consist of fusions with GCN4 leucine zipper-forming sequences.

Fig. 1. (*A*) Schematic representation of the strategy for generating a functional validation profile of a biochemical network by using the DHFR PCA. Positive clones are detected with the DHFR survival-selection assay. They correspond to interacting component proteins of two convergent signal transduction pathways (Path 1 and Path 2). An interaction matrix (upper left) represents all positive (green) and negative (red) interacting pairs observed in the survival-selection assay. Positive clones from survival selection are propagated and subjected to two functional analyses. First, with use of the DHFR fluorescence assay, interactions are probed with pathway-specific stimulators (1 and 2) and inhibitors (A and B). Pharmacological profiles are established on the basis of the pattern of response of individual interactions to stimulators and inhibitors, represented in the histograms. (Ordinate axes represent fluorescence intensity.) For example, stimulation of pathway 1 will augment all of the interactions composing that pathway. Inhibitor A will inhibit protein interactions downstream, but not upstream of its site of action in pathway 1. Second, cellular locations of the interactions are determined by fluorescence microscopy, also by use of the DHFR fluorescence assay. (*B*) Well established connections within RTK (growth factor-activated)- and FRAP-mediated pathways that control initiation of translation and sites of action of inhibitors of these pathways. Broken line indicates indirect action. PI3K, phosphatidylinositol-3-kinase.

DHFR Survival-Selection Assay. Chinese hamster ovary (CHO) DUKX-B11 (DHFR$^-$) cells were split 24 h before transfection at 8×10^4 in 12-well plates in α-MEM (Life Technologies, Grand Island, NY) enriched with dialyzed FBS (HyClone) and supplemented with 10 μg/ml of adenosine, deoxyadenosine, and thymidine (Sigma). Cells were transfected using Lipofectamine reagent (Life Technologies) according to the manufacturer's instructions. Forty-eight hours after the beginning of the transfection, cells were split at $\approx 5 \times 10^4$ in 6-well plates in selective

medium consisting of α-MEM enriched with dialyzed FBS but without addition of nucleotides. Cells were observed, for the appearance of colonies, for 5–21 days after incubation in selective medium. Only cells expressing fused interacting partners gave rise to colonies. A few surviving colonies were isolated for each transfection by trypsinizing in cloning cylinders and were grown individually up to confluence.
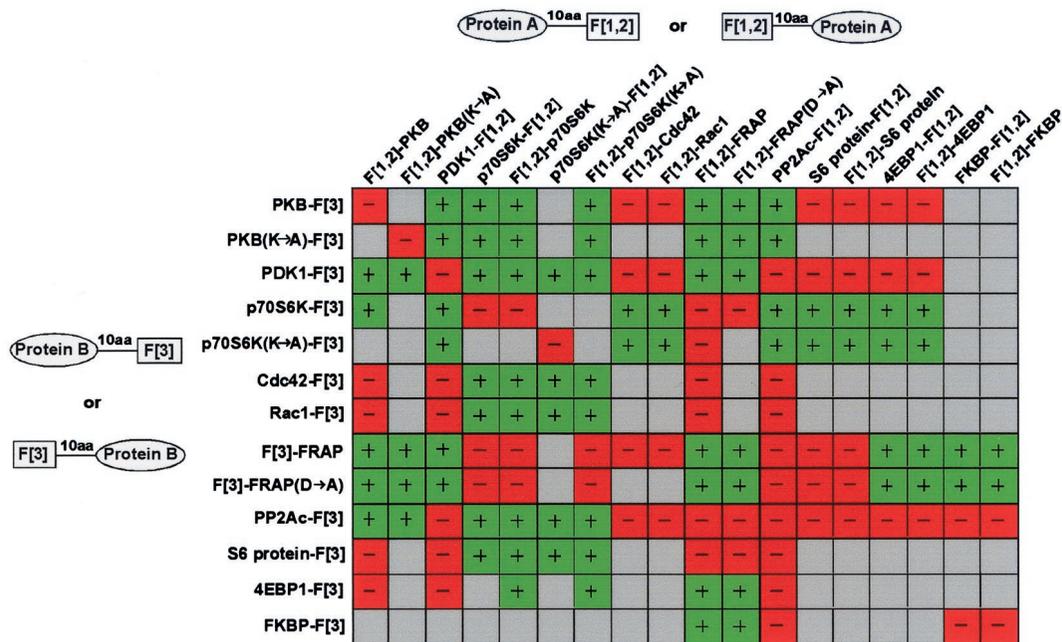
Fluorometric Analysis. CHO DUKX-B11 cells stably expressing interacting proteins fused to DHFR fragments were split at 2×10^5 in 12-wells plates in α-MEM (Life Technologies) enriched with dialyzed FBS (HyClone) and incubated for 24 h. Cells were washed with α-MEM and serum-starved (0.5% dialyzed FBS) in α-MEM containing 10 μM fluorescein-conjugated methotrexate (fMTX; Molecular Probes) for 20 h. Medium was removed, cells were washed, incubated in α-MEM containing 10 μM fMTX, but without serum, for 3 h, and untreated or treated with 20 μg/ml insulin (Roche Diagnostics) or 15% serum for 15 min. For the drug treatments, after the 20-h incubation, cells were pretreated with 20 nM rapamycin (Calbiochem) or 300 nM wortmannin (Calbiochem) for 3 h or 20 nM calyculin A (Calbiochem) for 45 min., and then 15% serum was added to the samples for 15 min. For all of the samples, medium was removed and the cells were washed and reincubated for 15 min in α-MEM (without fMTX), with the addition of drugs, insulin, or serum in corresponding samples, to allow for the efflux of unbound fMTX. The medium was removed, and the cells were washed one time with PBS and gently trypsinized. Plates were put on ice, and 100 μl of cold PBS was added to the cells. The total cell suspensions were transferred to 96-well white microtiter plates (Dynex, cat. no. 7905, VWR Scientific, Mount Royal, QC, Canada) and kept on ice before fluorometric analysis (Perkin–Elmer HTS 7000 BioAssay Reader). Afterward, the data were normalized to total protein concentration in cell lysates (Bio-Rad protein assay).

Fluorescence Microscopy. COS cells were grown on 18-mm glass cover slips to $\approx 2 \times 10^5$ in DMEM (Life Technologies) enriched with 10% cosmic calf serum (HyClone) in 12-well plates. Cells were transiently cotransfected with different combinations (as indicated) of the pMT3 plasmid harboring the full-length cDNAs fused by 10-aa linkers to F[1, 2] or F[3], using Lipofectamine (Life Technologies). Twenty-four hours after transfection, fMTX (Molecular Probes) was added to the cells at a final concentration of 10 μM. After an incubation of 20 h, medium was removed and cells were washed and reincubated for 15 min in DMEM enriched with 10% cosmic calf serum, to allow for the efflux of unbound fMTX. The medium was removed and cells were washed two times with cold PBS and finally mounted on glass slides. Fluorescence microscopy was performed on live cells with a Zeiss Axiophot microscope (objective lens Zeiss Plan Neofluar 100X/1.30).

Results and Discussion

Screening of Protein–Protein Interactions in the RTK/FRAP Pathways. The first step in our strategy was to screen proteins that are involved in RTK- and FRAP-mediated signaling for interactions among each other, with use of the simple DHFR survival-selection PCA. Prokaryotic and eukaryotic DHFR is central to cellular one-carbon metabolism and is absolutely required for cell survival. The principle of the survival assay is that cells simultaneously expressing complementary fragments of DHFR fused to interacting proteins or peptides will survive in media depleted of nucleotides, only if the proteins interact and then bring the complementary fragments of DHFR into proximity where they can fold and reassemble into active enzyme. For survival-selection studies, we used CHO DUKX-B11 (DHFR$^-$) cells stably cotransfected with various combinations of the fusions. Cotransfectants were selected for survival in nucleotide-

Protein A—10aa—F[1,2] or F[1,2]—10aa—Protein A

Protein B—10aa—F[3]
or
F[3]—10aa—Protein B

	F[1,2]-PKB	F[1,2]-PKB(K→A)	PDK1-F[1,2]	p70S6K-F[1,2]	F[1,2]-p70S6K	p70S6K(K→A)-F[1,2]	F[1,2]-p70S6K(K→A)	F[1,2]-Cdc42	F[1,2]-Rac1	F[1,2]-FRAP	F[1,2]-FRAP(D→A)	PP2Ac-F[1,2]	S6 protein-F[1,2]	F[1,2]-S6 protein	4EBP1-F[1,2]	F[1,2]-4EBP1	FKBP-F[1,2]	F[1,2]-FKBP
PKB-F[3]	−		+	+	+		+	−	−	+	+	+	−	−	−	−		
PKB(K→A)-F[3]		−	+	+	+		+			+	+	+						
PDK1-F[3]	+	+	−	+	+	+	+	−	−	+	+	−	−	−	−	−		
p70S6K-F[3]	+		+	−	−			+	+	−	−	+	+	+	+	+		
p70S6K(K→A)-F[3]			+			−		+	+	−		+	+	+	+	+		
Cdc42-F[3]	−		−	+	+	+	+			−		−						
Rac1-F[3]	−		−	+	+	+	+			−		−						
F[3]-FRAP	+	+	−	−		−	−	−	−	+	+	−	−		+	+	+	+
F[3]-FRAP(D→A)	+	+	+	−	−		−			+	+	−	−		+	+	+	+
PP2Ac-F[3]	+	+	−	+	+	+	+	−	−	−	−	−	−	−	−	−	−	−
S6 protein-F[3]	−		−	+	+	+	+			−	−	−						
4EBP1-F[3]	−		−	+		+				+	+							
FKBP-F[3]										+	+	−					−	−

Fig. 2. Summary of the results obtained for the different protein–protein interactions tested in the RTK/FRAP network with the DHFR survival-selection assay in CHO DUKX-B11 (DHFR⁻) cells. On the *x* axis are the fusions to DHFR[1,2] fragment, and on the *y* axis the fusions to DHFR[3] fragment. The orientations of the fusions (N-terminal or C-terminal) also are indicated. Positive interactions, green (+); absence of interaction, red (−); not tested, gray squares.

free medium (selection for DHFR activity). The survival-selection assay is extremely sensitive; we have previously demonstrated that only 25–100 molecules of reconstituted DHFR per cell are necessary for cell survival (4). DHFR⁺ cell lines can be used in a recessive selection strategy (6) or the screening for protein interactions could be achieved with the fluorescence assay. However, for the fluorescence studies described below, it was more convenient to work with a homogenous clonal population of cells expressing exogenous proteins at low levels.

Protein–protein interactions were tested with three variations of the protein DHFR fragment fusions. First, except in specific cases, we tested the same interactions with fusions of the test proteins at either the N or C terminus of DHFR fragments. We tested these variants because, not knowing the structures of these proteins, we would not be able to predict whether the complementary DHFR fragments could be brought into proximity because the individual C or N termini of the interacting test proteins are too far from each other. Second, we tested what we call a fragment-swapping control. We reasoned that if an interaction is observed with one protein-fragment configuration (e.g., X-F[1, 2] and Y-F[3]), swapping proteins and fragments should give the same result (i.e., Y-F[1, 2] and X-F[3]). These controls could preclude a remote source of false-positive signals. A specific protein-fragment fusion could possibly induce fragment complementation in the absence of interaction with a partner protein-fragment fusion by some alternative mechanism. For example, if a protein were to interact with the fused DHFR fragment in a way that induced the independent folding of the fragment, the folded fragment might act as a template for binding to the complementary fragment, independent of interaction between the test proteins. Such spontaneous complementation is a problem inherent in another approach for measuring protein–protein interactions based on β-galactosidase subunit complementation. In this approach, the prefolded subunits always interact to some extent, leading to a false-positive signal of an amplitude dependent on protein expression levels (10). This problem does not occur with the DHFR PCA because the fragments are incapable of folding independently (6, 11). Third,

we also tested "kinase-dead" forms of some of the protein kinases studied here. These mutants, by acting as "substrate traps," are thought to bind with higher affinity to their substrates.

A total of 148 combinations of 35 different protein–protein interactions in the RTK/FRAP signal transduction pathways were tested against each other (Fig. 2). In all cases, full-length protein-DHFR fragment fusions were expressed. Of the 35 interactions tested, 14 corresponded to interacting partners. Nine of these interactions have been identified previously. However, we were surprised to find five additional interactions that had not been reported previously or had only been inferred, on the basis of indirect evidence. We discuss these in detail below. Growth rates for colonies of clones expressing differently oriented fusions were not significantly different, suggesting that the linker length was sufficiently long to allow proteins to interact and for the DHFR fragments to be brought into proximity to fold/reassemble. We used a flexible linker peptide of 10 aa between the proteins and DHFR fragments, allowing us to probe interactions across distances of 80 Å (≈4 Å per peptide bond × 10 aa × 2 linkers: 1 per fusion). When we tested the substrate-trapping mutants of protein kinases, we observed no difference in the growth rates of these compared with the wild-type, active kinases. The dissociation constants for kinase–substrate interactions are low (≈10 nM to 10 μM) (12), and these values are well within the range of detection of the DHFR survival PCA (4).

Pharmacological Profiles and Cellular Location of Interacting Proteins. As discussed in the Introduction, our goal was to demonstrate that the DHFR PCA could be used to simultaneously screen and functionally validate protein–protein interactions. Two functional validation experiments were envisioned (Fig. 1*A*): (*i*) experiments that would allow the measurement of the effects of pathway-specific stimulators and inhibitors on individual protein–protein interactions in a signaling cascade and (*ii*) experiments that would allow for the unambiguous determination of the physical location of the interaction. It is possible to obtain both types of information with a fluorescence DHFR PCA. The
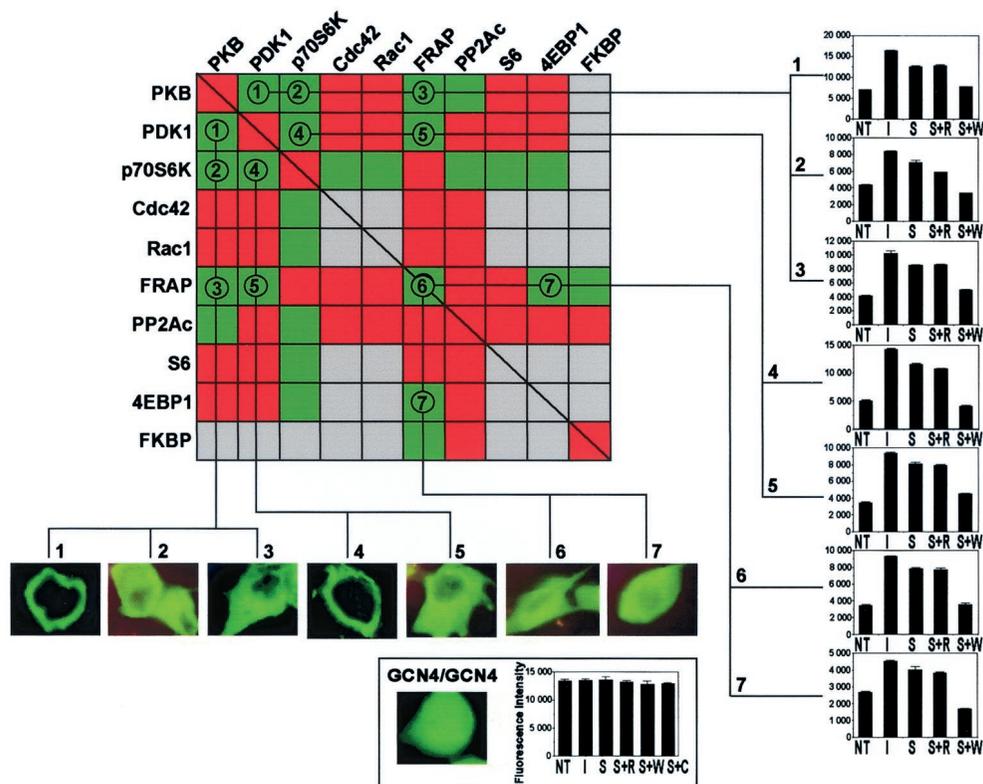
Fig. 3. Fluorometric and microscopic analysis of the wortmannin-sensitive/rapamycin-resistant components of the network. The grid represents all positive (green) and negative (red) interactions observed in survival selection. The pharmacological profiles are represented by the histograms (right). Cells were treated with stimulants and inhibitors as described in *Materials and Methods* (x axis; NT, no treatment; I, insulin; S, serum; R, rapamycin; W, wortmannin). Fluorescence intensity is given in relative fluorescence units (y axis). The background fluorescence corresponding to nontransfected cells was subtracted from the fluorescence intensities of all of the samples. Error bars represent standard errors for the mean calculated from at least three independent experiments. Microscopy revealing patterns of locations also is presented. The dimerization of GCN4 leucine zipper (GCN4/GCN4) is used as a control. The fusion protein pairs used in these experiments were: PDK1-F[1,2]/PKB-F[3], F[1,2]-p70S6K/PKB-F[3], F[1,2]-FRAP/PKB-F[3], F[1,2]-p70S6K/PDK1-F[3], PDK1-F[1,2]/F[3]-FRAP, F[1,2]-FRAP/F[3]-FRAP, F[1,2]-FRAP/4EBP1-F[3], and F[1,2]-GCN4/GCN4-F[3].

basis of this assay is that complementary fragments of DHFR, when expressed and reassembled in cells, will bind with high affinity ($K_d = 540$ pM) to fMTX in a 1:1 complex. fMTX is retained in cells by this complex, whereas the unbound is actively and rapidly transported out of the cells (4, 5). Thus, the fluorescence signal measured in an intact living cell is a direct stoichiometric measure of the number of molecules of reconstituted DHFR and, by inference, the number of interacting protein complexes. Fluorescence can be measured by any standard spectroscopic technique, including fluorescence-activated cell sorting (FACS) or spectroscopy. The locations of the complexes within a cell can be monitored by simple florescence microscopy. Because the observed fluorescence arises from 1:1 complexes of fMTX and reconstituted DHFR, the location of the fluorescence in the cell represents the location of the interacting protein complexes.

Insulin- and serum-induced signaling have been studied in detail in CHO cells (13), and biochemical analyses of insulin receptor-mediated and serum-induced RTK/FRAP pathways are well documented (for review, see ref. 14). We restricted the pathway inhibitors used in these studies to three small molecules: wortmannin, which inhibits PI-3K; rapamycin, a specific inhibitor of FRAP; and calyculin A, an inhibitor of the serine/threonine phosphatase PP2A. We chose these inhibitors because their sites and mechanisms of action are well known and because they act at key points in the pathways studied (Fig. 1B). Specifically, wortmannin acts upstream of all of the interactions we studied in the RTK pathway, but should have no effect on

interactions downstream of FRAP. In contrast, rapamycin should affect all interactions downstream of FRAP. Both drugs would be predicted to inhibit protein–protein interactions that are downstream of both the RTK and FRAP pathways (e.g., p70S6K with S6 protein, Fig. 1B). Calyculin A is a specific inhibitor of PP2A and thus should interfere with the interactions between PP2A and its substrates.

Fluorometric experiments were performed as described in *Materials and Methods* by using the stable cells derived from the survival-selection screening described above. The fluorescence spectroscopy results on living cells fell into two categories, based on distinct pharmacological profiles: (*i*) insulin- and serum-stimulated and wortmannin-inhibited interactions (Fig. 3) and (*ii*) rapamycin-sensitive interactions (Fig. 4). As we expected, all interactions downstream of insulin- or serum-activated signal transduction pathways responded to these stimuli and all were blocked by wortmannin.

For example, we observed a direct interaction between PDK1 and PKB. PDK1 has been identified as a specific PKB kinase (for review, see refs. 15 and 16). Further, fluorescence microscopy results showed that the interaction between PDK1 and PKB occurs exclusively at the plasma membrane (Fig. 3, 1). It has been proposed that membrane localization of both enzymes is required for PKB phosphorylation by PDK1, via binding to phosphatidylinositol 3,4,5-trisphosphate (PIP$_3$) through pleckstrin homology domains of both kinases. PDK1/PKB interaction is an early step in RTK pathways and therefore the membrane association of the complex is consistent both with known mo-
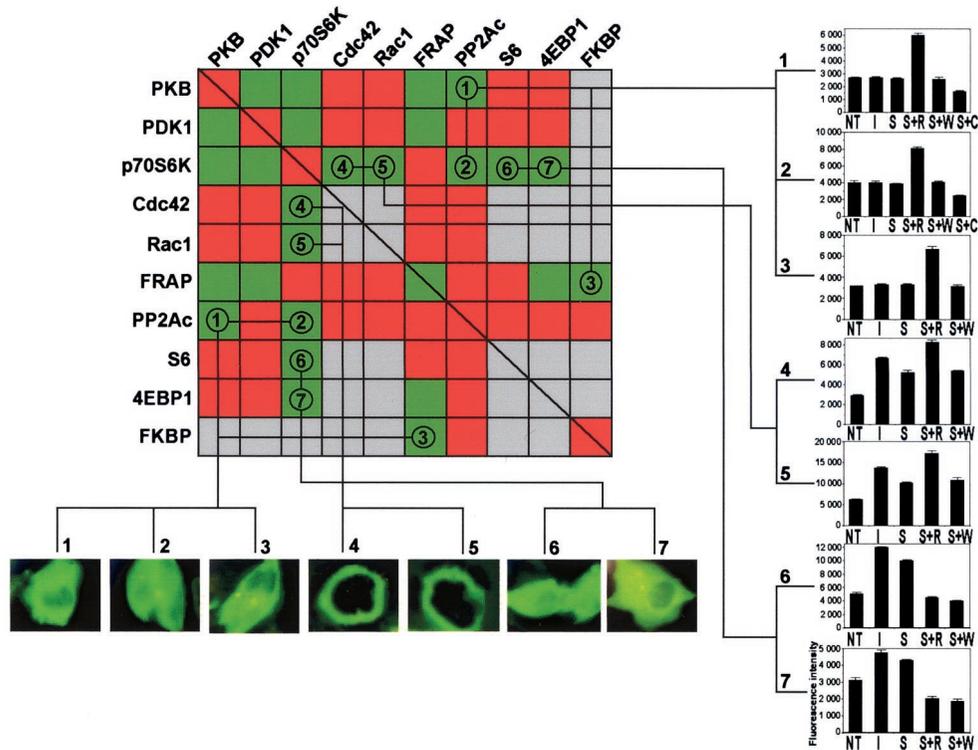
Fig. 4. Fluorometric and microscopic analysis of the rapamycin-sensitive components of the network (C, calyculin A; see legend to Fig. 3 for all other abbreviations). The fusion protein pairs used in these experiments were: PP2A-F[1,2]/PKB-F[3], PP2A-F[1,2]/p70S6K-F[3], F[1,2]-FRAP/FKBP-F[3], F[1,2]-Cdc42/P70S6K-F[3], F[1,2]-Rac1/p70S6K-F[3], F[1,2]-p70S6K/S6-F[3], and F[1,2]-p70S6K/4EBP1-F[3].

lecular mechanisms of localization and with the pathway hierarchy. p70S6K is also a substrate of PDK1 (17, 18), and predictably, the pharmacological profile and cellular locations of this interaction were identical to those of PDK1/PKB (Fig. 3, 4). We also observed a direct interaction between PKB and p70S6K with the same pharmacological profile as PDK1/PKB, but with a cytosolic distribution (Fig. 3, 2). This interaction had been suspected but never demonstrated before, and PKB has not been shown to act as a p70S6K kinase *in vitro* (19).

Recent studies suggest that the RTK and FRAP pathways are not entirely independent, and our results are consistent with the view that considerable cross-talk occurs between the two pathways. For instance, we observed not only a direct and previously known interaction between PKB and FRAP (ref. 20; Fig. 3, 3), but also an interaction between PDK1 and FRAP (Fig. 3, 5). Both showed identical pharmacological profiles and cellular locations. We also observed insulin- and serum-induced homodimerization of FRAP (Fig. 3, 6). Because homodimerization is induced by insulin and serum and inhibited by wortmannin, FRAP homodimerization might be activated by PDK1 and/or PKB. The observed interaction between FRAP and 4EBP1 is consistent with studies showing that FRAP can directly phosphorylate 4EBP1 *in vitro* (refs. 21 and 22; Fig. 3, 7). However, this interaction has the same pharmacological profiles as others in the RTK pathway, again suggesting that RTK pathways may mediate this interaction directly through FRAP.

Rapamycin-sensitive protein–protein interactions showed three distinct pharmacological profiles (Fig. 4). The first profile (1, 2, and 3) consisted of interactions insensitive to insulin, serum, and wortmannin, but enhanced by rapamycin. These include the well known, rapamycin-induced cytosolic interaction between FKBP and FRAP (refs. 7 and 23; Fig. 4, 3); the recently described interaction of the serine/threonine phosphatase PP2A with p70S6K (ref. 30; Fig. 4, 2); and an inferred interaction of

PP2A with PKB (ref. 24; Fig. 4, 1). Moreover, the complexes were partially inhibited by the PP2A-specific inhibitor calyculin A, suggesting that the interaction occurs in part between the
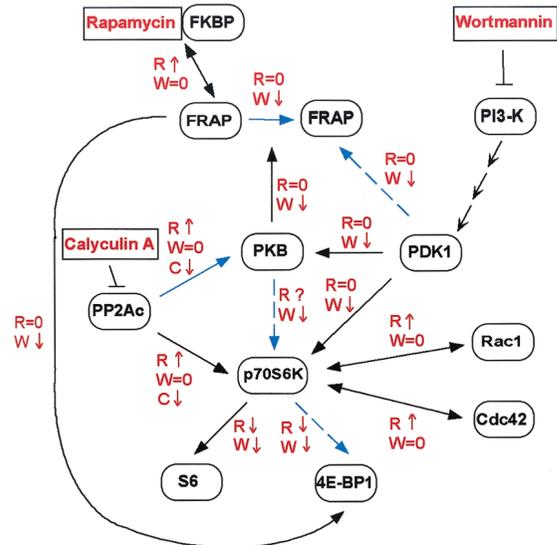
Fig. 5. Summary of the protein–protein interactions involved in the RTK/FRAP network and their responses to inhibitors. This summary is based on the results obtained from survival-selection and pharmacological profile experiments. The effects of each drug are indicated (C, calyculin A; R, rapamycin; W, wortmannin). The blue arrows indicate protein–protein interactions that have not been previously observed. Single-head arrows indicate kinase- or phosphatase-substrate catalytic events. Double-head arrows represent equilibrium noncatalytic interactions. Broken arrows indicate that the nature of the interactions is unknown.

catalytic site of PP2A and substrate sites on p70S6K and PKB. Evidence from genetic and biochemical studies of yeast and mammalian cells suggests that the actions of FRAP are mediated indirectly through PP2A. Specifically, it has been proposed that FKBP/rapamycin sterically prevents the phosphorylation by FRAP of an inhibitory subunit of PP2A (25, 26), resulting in dissociation of the inhibitory and catalytic subunits of the phosphatase, which thereby allows PP2A to dephosphorylate and deactivate p70S6K. Our results are consistent with this model, placing the interaction of PP2A with p70S6K downstream of the FKBP/rapamycin/FRAP complex. A similar mechanism acting on PKB also is supported by our results.

A second profile supports a model for membrane anchoring of p70S6K at the membrane surface by the Rho family GTPases Cdc42 (Fig. 4, 4) and Rac1 (Fig. 4, 5) (27). Both of these interactions could occur at the plasma membrane. p70S6K contains no known membrane-anchoring domains, and yet interactions with a kinase known to activate it (PDK1) occur at the plasma membrane (Fig. 3, 4). The pharmacological profiles were identical for both interactions: rapamycin enhanced the serum-induced association, whereas wortmannin had no effect. Our results can be interpreted in the same way as for rapamycin effects on the p70S6K/PP2A interaction: in the presence of rapamycin; PP2A is activated, resulting in hypophosphorylation and translocation of p70S6K to the membrane through direct interactions with Cdc42 and Rac1.

Finally, the downstream interaction of p70S6K/S6 protein is affected by all drugs and stimulants, defining a third profile (Fig. 4, 6) and a point of convergence of the two pathways (× in Fig. 1*A*). However, we also observed an interaction between p70S6K and 4EBP1, which has the same pharmacological profile and cytosolic location as p70S6K/S6 (Fig. 4, 7). There is no evidence that 4EBP1 is a substrate of p70S6K *in vitro*; however, 4EBP1 has been shown to be phosphorylated on multiple residues *in vivo* and rapamycin prevents phosphorylation of some of these sites (28, 29). Further, dephosphorylation of 4EBP1 in response to rapamycin is mediated indirectly by PP2A (30). Our results suggest that the direct link between PP2A and 4EBP1 may be dephosphorylation and inactivation of p70S6K by PP2A.

We have demonstrated a simple and sensitive assay to select clonal populations of cells in which a specific interacting pair of proteins is expressed. Further, the pharmacological profiles and cellular location of interactions allowed us to "place" each gene product at its relevant point in the pathways. From the results of our analysis, a map of the organization of the RTK/FRAP network has emerged, which is consistent with existing models for the organization of the pathway, but includes interactions discovered that should be explored in more detail (Fig. 5). The ability to monitor a network of protein interactions in living cells containing components of the underlying pathway studied here revealed hidden connections, not observed before, despite intense scrutiny of this network. Further, such analysis is not limited to a specific cell type; we have already demonstrated the utility of PCA strategies in bacteria and mammalian cells (3–6). The results presented here demonstrate that PCA has the features necessary to perform validation and pathway-mapping strategy for a general protein function.

1. Fields, S. & Song, O. (1989) *Nature (London)* **340,** 245–246.
2. Uetz, P., Giot, L., Cagney, G., Mansfield, T. A., Judson, R. S., Knight, J. R., Lockshon, D., Narayan, V., Srinivasan, M., Pochart, P., *et al.* (2000) *Nature (London)* **403,** 623–627.
3. Pelletier, J. N., Campbell-Valois, F. & Michnick, S. W. (1998) *Proc. Natl. Acad. Sci. USA* **95,** 12141–12146.
4. Remy, I. & Michnick, S. W. (1999) *Proc. Natl. Acad. Sci. USA* **96,** 5394–5399.
5. Remy, I., Wilson, I. A. & Michnick, S. W. (1999) *Science* **283,** 990–993.
6. Michnick, S. W., Remy, I., Campbell-Valois, F.-X., Vallee-Belisle, A. & Pelletier, J. N. (2000) *Methods Enzymol.* **328,** 208–230.
7. Sabatini, D. M., Erdjument-Bromage, H., Lui, M., Tempst, P. & Snyder, S. H. (1994) *Cell* **78,** 35–43.
8. Brown, E. J., Albers, M. W., Shin, T. B., Ichikawa, K., Keith, C. T., Lane, W. S. & Schreiber, S. L. (1994) *Nature (London)* **369,** 756–758.
9. Kaufman, R. J., Davies, M. V., Pathak, V. K. & Hershey, J. W. (1989) *Mol. Cell. Biol.* **9,** 946–958.
10. Rossi, F., Charlton, C. A. & Blau, H. M. (1997) *Proc. Natl. Acad. Sci. USA* **94,** 8405–8410.
11. Gegg, C. V., Bowers, K. E. & Matthews, C. R. (1997) *Protein Sci.* **6,** 1885–1892.
12. Bhalla, U. S. & Iyengar, R. (1999) *Science* **283,** 381–387.
13. Mamounas, M., Gervin, D. & Englesberg, E. (1989) *Proc. Natl. Acad. Sci. USA* **86,** 9294–9298.
14. Avruch, J. (1998) *Mol. Cell. Biochem.* **182,** 31–48.
15. Belham, C., Wu, S. & Avruch, J. (1999) *Curr. Biol.* **9,** R93–R96.
16. Vanhaesebroeck, B. & Alessi, D. R. (2000) *Biochem. J.* **3,** 561–576.
17. Alessi, D. R., Kozlowski, M. T., Weng, Q. P., Morrice, N. & Avruch, J. (1998) *Curr. Biol.* **8,** 69–81.
18. Pullen, N., Dennis, P. B., Andjelkovic, M., Dufner, A., Kozma, S. C., Hemmings, B. A. & Thomas, G. (1998) *Science* **279,** 707–710.
19. Dufner, A., Andjelkovic, M., Burgering, B. M., Hemmings, B. A. & Thomas, G. (1999) *Mol. Cell. Biol.* **19,** 4525–4534.
20. Nave, B. T., Ouwens, M., Withers, D. J., Alessi, D. R. & Shepherd, P. R. (1999) *Biochem. J.* **2,** 427–431.
21. Brunn, G. J., Hudson, C. C., Sekulic, A., Williams, J. M., Hosoi, H., Houghton, P. J., Lawrence, J., Jr., & Abraham, R. T. (1997) *Science* **277,** 99–101.
22. Gingras, A. C., Gygi, S. P., Raught, B., Polakiewicz, R. D., Abraham, R. T., Hoekstra, M. F., Aebersold, R. & Sonenberg, N. (1999) *Genes Dev.* **13,** 1422–1437.
23. Lorenz, M. C. & Heitman, J. (1995) *J. Biol. Chem.* **270,** 27531–27537.
24. Andjelkovic, M., Jakubowicz, T., Cron, P., Ming, X. F., Han, J. W. & Hemmings, B. A. (1996) *Proc. Natl. Acad. Sci. USA* **93,** 5699–5704.
25. Di Como, C. J. & Arndt, K. T. (1996) *Genes Dev.* **10,** 1904–1916.
26. Jiang, Y. & Broach, J. R. (1999) *EMBO J.* **18,** 2782–2792.
27. Chou, M. M. & Blenis, J. (1996) *Cell* **85,** 573–583.
28. Heesom, K. J., Avison, M. B., Diggle, T. A. & Denton, R. M. (1998) *Biochem. J.* **336,** 39–48.
29. Gingras, A. C., Kennedy, S. G., O'Leary, M. A., Sonenberg, N. & Hay, N. (1998) *Genes Dev.* **12,** 502–513.
30. Peterson, R. T., Desai, B. N., Hardwick, J. S. & Schreiber, S. L. (1999) *Proc. Natl. Acad. Sci. USA* **96,** 4438–4442.

BIOCHEMISTRY